Proceedings of the 12th International Conference on
Aluminium Alloys, September 5-9, 2010, Yokohama, Japan

pp. 389-394

Strengthening of 6xxx Series Sheet Alloys During Natural Ageing and Early-stage Artificial Ageing

Paul A. Rometsch[1], Lingfei Cao[1] and Barry C. Muddle[1]
[1]ARC Centre of Excellence for Design in Light Metals, Monash University, VIC 3800, Australia

The strengthening mechanisms during natural ageing and early-stage artificial ageing have been investigated for Al-Mg-Si(-Cu) sheet alloys using primarily tensile testing, transmission electron microscopy (TEM) and 3-dimensional atom probe (3DAP) analysis. The focus of this study is on understanding the hardening behaviour in terms of the various distributions of clusters, coherent zones and/or precipitates. Analysis of 3DAP data reveals high number densities of very small clusters, causing the particle size distribution to be heavily skewed towards small clusters both in naturally-aged conditions and also in some artificially-aged conditions. In terms of volume fractions of differently sized solute aggregates, the size distribution is influenced more by the ageing conditions such that natural ageing gives high volume fractions of small clusters, while artificial ageing after short natural ageing times increases the volume fraction of larger solute aggregates. Microstructural data such as volume fractions and Mg/Si ratios of the variously sized solute aggregates are related to the yield strength for a range of naturally aged and under-aged conditions and thus utilised to better understand the early-stage strengthening behaviour of these alloys.

Keywords: *6xxx, natural ageing, 3DAP, strengthening.*

1. Introduction

Strengthening of age hardening aluminium alloys has generally been ascribed to and modelled in terms of a combination of the 'intrinsic' strength of the material, the solid solution strengthening contribution and the precipitation strengthening contribution [1, 2]. More recently, however, it has been demonstrated that clustering of solute atoms can contribute significantly to the strengthening of Al-Mg-Si-Cu alloys, especially in the naturally aged and under-aged conditions, and should therefore be included in any strengthening model in addition to the other strengthening contributions [3, 4]. Although these 'clusters' are often too small to be resolved by TEM, analysis by 3DAP can provide further insights into the nature of the variously sized solute aggregates [5, 6].

Based on 3DAP and TEM results, Buha *et al* [7-8] have approximately categorised solute aggregates into (a) irregularly shaped co-clusters with about 10-30 detected solute atoms, (b) spherical zones with about 30-100 detected solute atoms, and (c) elongated β'' precipitates with typically more than 100 detected solute atoms. Although there is still controversy about the various terminologies and about exactly what constitutes clusters, zones and precipitates (all termed solute aggregates in the current work), the categories from Buha *et al* [7, 8] are taken as a convenient, if approximate, starting place for the current investigation. Since little is known about the relative strengthening contributions of these different solute aggregates, the purpose of this work is to investigate how the nature and size-distributions of the various types of solute aggregates affect the yield strength of two Al-Mg-Si(-Cu) alloys in various naturally-aged and under-aged conditions.

2. Experimental Methods

The chemical compositions of the two 6xxx series alloys investigated in this work are given in Table 1. The alloys were DC-cast, homogenised and hot and cold rolled to 1 mm thick sheets. All samples were solution treated for 0.5 h in a salt bath at 550°C, quenched into room temperature water and then either naturally aged only (designated as T4) or aged for 0.5 h in an oil bath at 170°C after various times of prior natural ageing (designated as T6). Tensile testing was carried out on samples with a cross-sectional area of 5 mm^2 and a gauge length of 20 mm using an Instron 4505 tensile machine at an extension rate of 1.0 mm/min. 3DAP analysis was performed using an Oxford NanoScience three dimensional atom probe field ion microscope under ultrahigh vacuum conditions (about $3x10^{-11}$mbar) with a pulse fraction of 20%, at a specimen temperature of 25 K, and with a detector efficiency of 45%. Analysis of the 3DAP data was carried out on 1-2 boxes from each dataset (one needle per condition) using PoSAP software, with the minimum distance between atoms (D), the surround distance (L) and the erosion distance (S) all set to 0.5 nm. A value of N = 2 was chosen for the minimum number of detected solute atoms per aggregate (N) so as to give more information about small clusters [9]. Both 3DAP needles and TEM foils were prepared with standard electro-polishing techniques. TEM was carried out with a Phillips CM20 transmission electron microscope at 200 kV.

Table 1: Chemical compositions of the two aluminium alloys

Alloy		Si	Mg	Cu	Fe	Mn	Cr	Zn	Ti
Alloy 1	wt%	1.35	0.58	0.04	0.14	0.04	0.10	0.21	0.10
	at%	1.30	0.65	0.02	0.07	0.02	0.05	0.09	0.06
Alloy 2	wt%	1.07	0.48	0.29	0.12	0.06	0.08	0.19	0.01
	at%	1.03	0.54	0.12	0.06	0.03	0.04	0.08	0.01

3. Results and Discussion

3.1 Alloy 1

The results in Fig. 1 illustrate the detrimental effect of natural ageing for Alloy 1. Within as little as 3 h of natural ageing before artificially ageing for 0.5 h at 170°C, the T6 yield strength dropped by more than 100 MPa compared to samples with negligible prior natural ageing. While the coarser microstructure in Fig 1(a) clearly corresponds to a higher strength, increasing the prior natural ageing time from 3 h to 168 h hardly changes the yield strength and the microstructure.

The 3DAP results in Fig. 2(a) confirm the Fig. 1 findings that the T6 sample with a yield strength of 262 MPa has a significantly higher volume fraction of larger solute aggregates with >100 detected atoms than the lower strength samples do (here in the T4 condition). Natural ageing, on the other

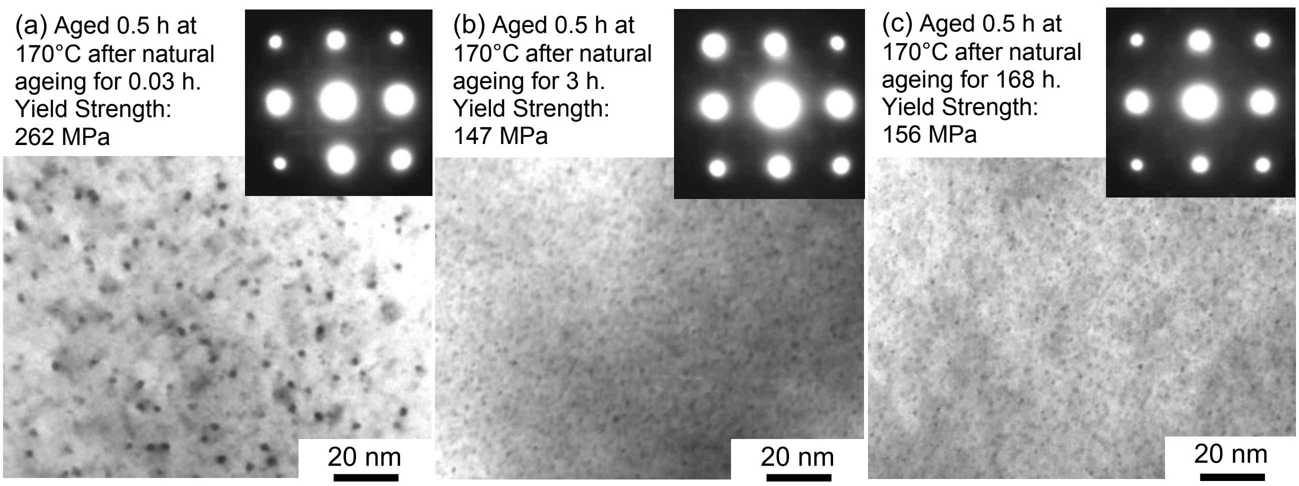

Fig. 1: Bright field TEM micrographs (and associated $[001]_{Al}$ diffraction patterns) of Alloy 1 showing the effect of natural ageing on the artificially aged size-distributions of solute aggregates, along with corresponding yield strengths. The alloy contains large coherent zones and small early-stage β'' precipitates in the higher strength condition (a), but mainly a fine distribution of coherent zones in the two lower strength conditions (b) and (c).

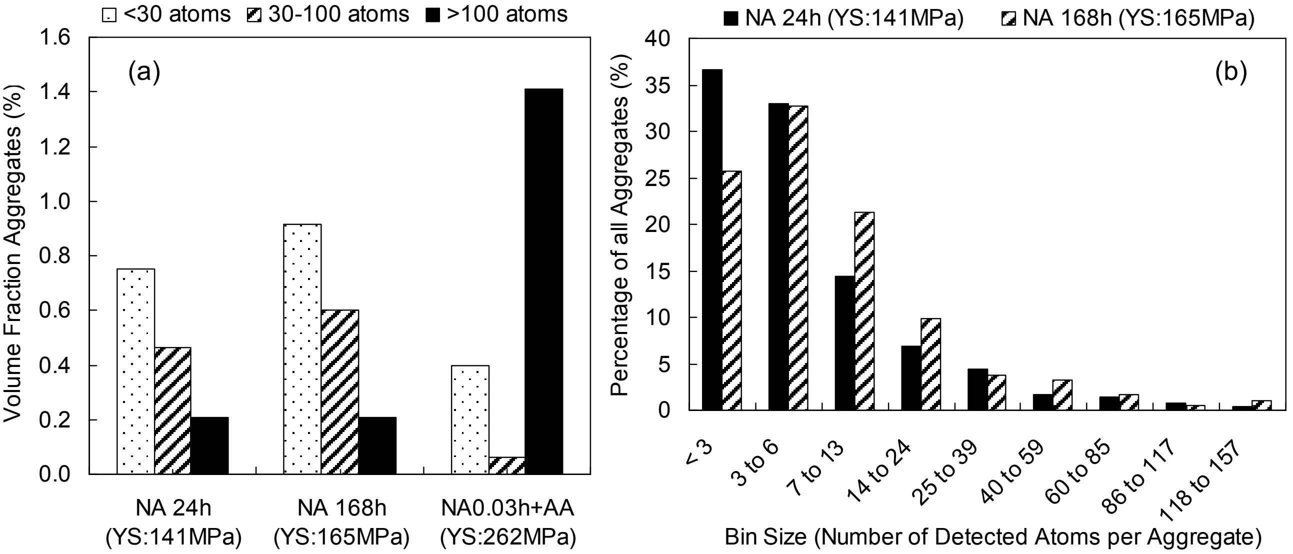

Fig. 2: 3DAP analysis results and corresponding yield strengths for Alloy 1 naturally aged for 24 h and 168 h. (a) Volume fractions of variously sized solute aggregates with NA0.03h+AA results (aged 0.5 h at 170°C after 0.03 h of natural ageing) shown for comparison. (b) Histogram showing particle size distributions for natural ageing times of 24 h and 168 h. In each case, the aggregates include detected Mg+Si+Cu+Al atoms, with the smallest aggregates of 2 atoms containing no Al since N = 2.

hand, increases the T4 strength by increasing the amount of smaller aggregates in both the <30 atoms and 30-100 atoms categories, but not the larger aggregates. The histogram in Fig. 2(b) suggests that the 24 MPa higher T4 yield strength resulting from longer natural ageing is largely due to a change in the aggregate size-distribution towards larger aggregates after longer natural ageing times. Although the categories in Fig. 2 do not match those of Buha *et al* [7, 8] exactly, since the latter are based on a detection efficiency of 60% and a counting of solute atoms only, it could nevertheless be argued from the adapted methodology that a possible boundary between clusters and coherent zones may occur at close to 75 detected atoms (Mg+Si+Cu+Al) in Fig. 2. All these results indicate that, whilst large zones and precipitates are associated with high strengths, a strengthening contribution from clusters cannot be ignored.

3.2 Alloy 2

Figure 3(a) shows the effect of natural ageing on the yield strength of the Cu-containing Alloy 2 in both the T4 and T6 conditions. In addition, the corresponding average and maximum detected solute aggregate sizes are shown in Fig 3(b) to exhibit a similar trend with natural ageing time as the yield strength does. Based on a detection efficiency of 45%, the largest solute aggregate with 790 detected atoms corresponds to a total of 1756 atoms in reality (Mg+Si+Cu+Al), which, according to the categorisation of Buha *et al* [8] would be considered to be a β'' precipitate. The largest T6 solute aggregate after 720 h of prior natural ageing (with 205 detected total atoms) would, according to the categorisation of Buha *et al* [8], be considered to be a large zone comprised in reality of a total of 456 atoms (Mg+Si+Cu+Al). These predictions are in line with TEM results, which, for Alloy 2 are very similar to those in Fig. 1 [9]. Other elements such as Fe, Mn, Cr and Zn were very rarely, if ever, detected in solute aggregates and are therefore assumed not to play an important role in clustering.

Figure 4 shows the effect of natural ageing on the volume fraction of solute aggregates in both the T4 and T6 conditions. Whilst the increase in volume fraction with increasing natural ageing time in the T4 condition matches the trend in yield strength, the trend in T6 volume fraction correlates better with the yield strength when only larger solute aggregates with ≥23 atoms are considered. This was investigated further by grouping solute aggregates into five size categories as outlined in Table 2.

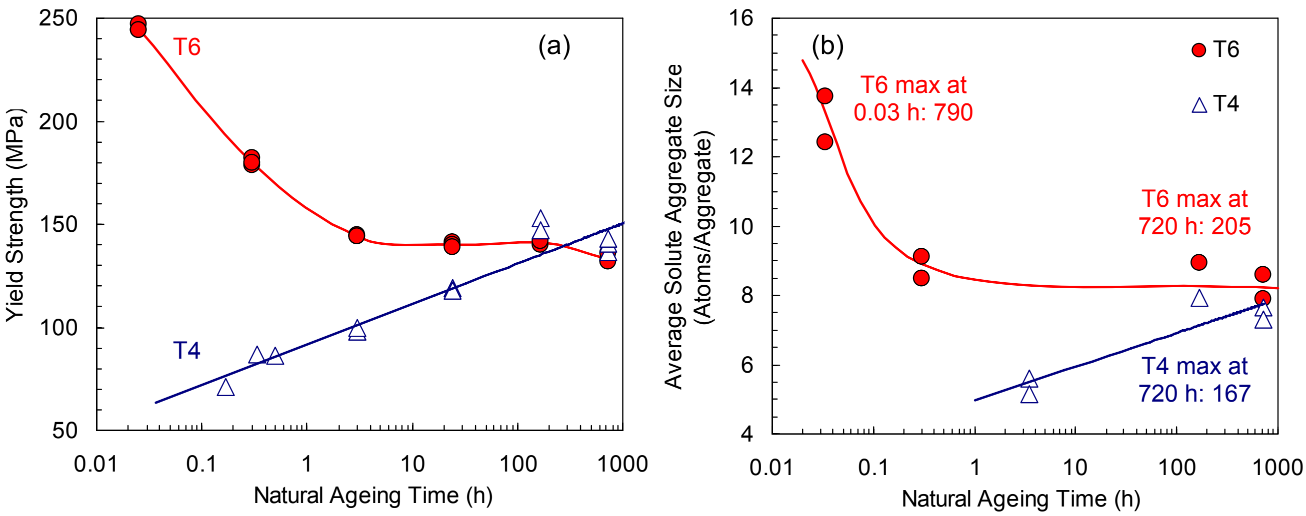

Fig. 3: Effect of natural ageing on (a) yield strength, and (b) average and maximum detected solute aggregate sizes in both the T4 condition and after subsequent ageing for 0.5 h at 170°C (T6). Use of N>2 would shift the curves in (b) to larger aggregate sizes but maintain similar trends.

These groupings are loosely based on those of Buha *et al* [8], but count total detected atoms per aggregate (rather than solute atoms only) and include more categories for smaller clusters. Since the strength of shearable particles is typically related to both the volume fraction and the particle radius [1-3], the categories were designed to vary linearly with the radius (i.e. $\propto \sqrt[3]{volume}$) while also attempting to identify different types of solute aggregates. The results from this analysis are presented in Table 3 and Figs. 5-6, and confirm that significant amounts of small solute aggregates (i.e. clusters with ≤75 detected atoms) exist in all investigated heat treatment conditions. The volume fraction of such clusters increases with natural ageing time in both T4 and T6 conditions, except that the quantity of the smallest clusters (Cluster 1) decreases with increasing natural ageing time in the T4 condition. Together with the results in Fig. 2(b), these results suggest that it may be better to view Cluster 1 as randomly arranged atoms in the solid solution rather than as distinct clusters. The dip in the T6 volume fraction curve in Fig. 4 arises from the combined effects of the variously sized solute aggregates illustrated in Fig. 5(a). The decreasing T6 yield strength with increasing natural ageing time in Fig. 3(a) therefore appears to correlate with both the decreasing amount of large aggregates (especially precipitates) and the simultaneously increasing amount of small aggregates. The increase in T4 yield strength with increasing natural ageing time, on the other hand, can be ascribed to the increasing volume fractions of Cluster 2, Cluster 3 and zones.

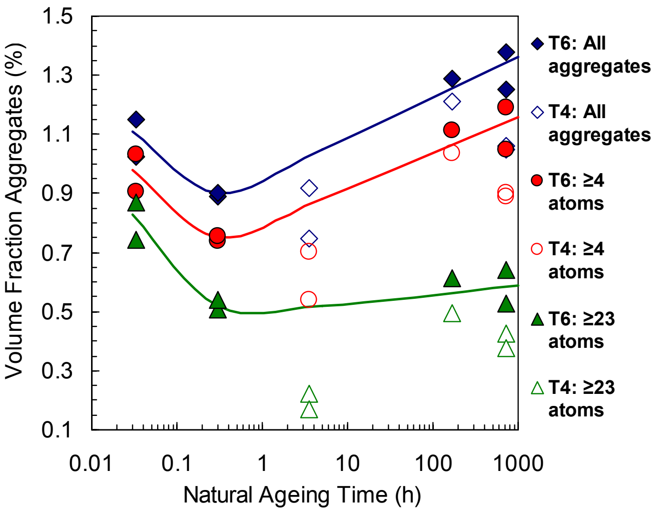

Fig. 4: Effect of natural ageing on total volume fractions of variously sized solute aggregates in T4 and T6 conditions (curves show T6 trends).

Table 2: Categorisation of variously sized solute aggregates, counting the sum of Mg+Si+Cu+Al

Number of Detected Atoms (45% Detection)	Actual Number of Atoms	Type of Solute Aggregate	Morphology
2 to 3	<7	Cluster 1	Irregular
4 to 22	7 to 50	Cluster 2	Irregular
23 to 75	51 to 166	Cluster 3	Irregular
76 to 225	167 to 500	Coherent Zone	~Spherical
>225	>500	Precipitate	Elongated

Table 3: Summary of 3DAP analysis results showing numbers of differently sized aggregates per box

Temper	Natural Ageing Time (h)	Box Size (nmxnmxnm)	Detected Atoms in Box	Detected Atoms in all Aggregates	Number of Differently Sized Aggregates in Analysis Box					
					All Aggregates	2 to 3 Atoms	4 to 22 Atoms	23 to 75 Atoms	76 to 225 Atoms	>225 Atoms
T6	0.03	10x11x150	965770	9895	797	523	235	11	18	10
T6	0.03	12x12x70	622573	7165	521	331	158	13	11	8
T6	0.3	12x13x225	2137317	19003	2242	1421	713	78	19	11
T6	0.3	12x13x70	628016	5651	619	392	196	21	6	4
T6	168	9x9x70	340238	4385	490	266	198	16	9	1
T6	720	6.5x10.5x150	650498	8976	1046	537	431	63	15	0
T6	720	7x11.5x70	353774	4426	560	301	221	30	8	0
T4	3.5	12.5x12.5x70	651758	5982	1066	618	413	33	2	0
T4	3.5	12.5x12.5x240	2140713	15982	3099	1931	1084	79	5	0
T4	168	7.8x8.1x70	273414	3320	418	209	180	24	5	0
T4	720	11x5x100	354542	3761	492	247	216	25	4	0
T4	720	11x5x70	247928	2595	356	172	163	20	1	0

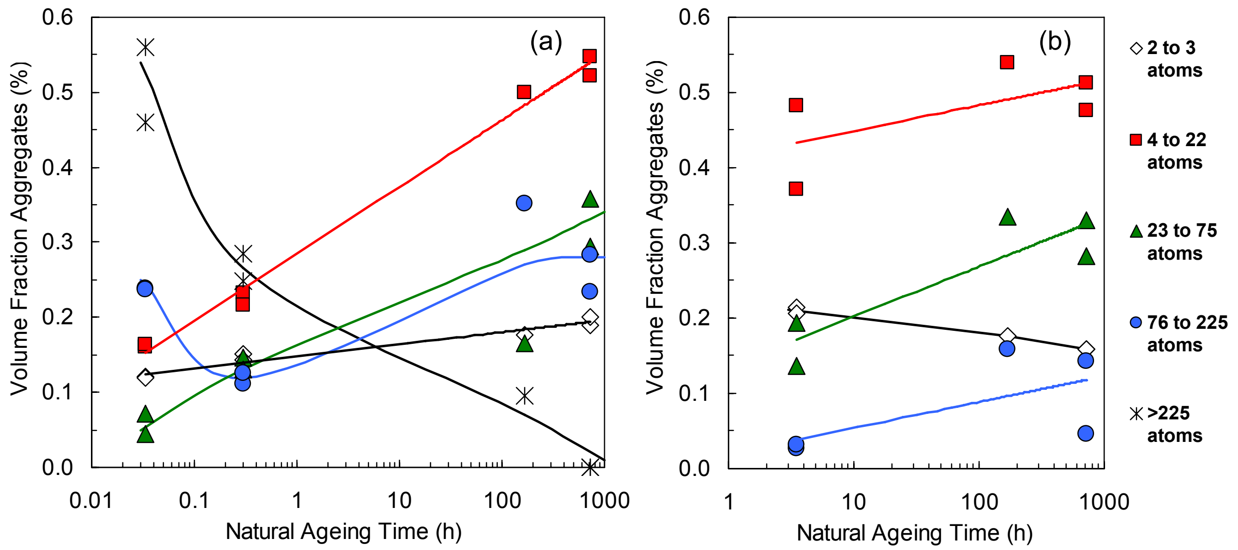

Fig. 5: Effect of natural ageing on the volume fraction of variously sized solute aggregates in (a) T6 and (b) T4 conditions, based on atoms in aggregates divided by the total number of atoms in the box.

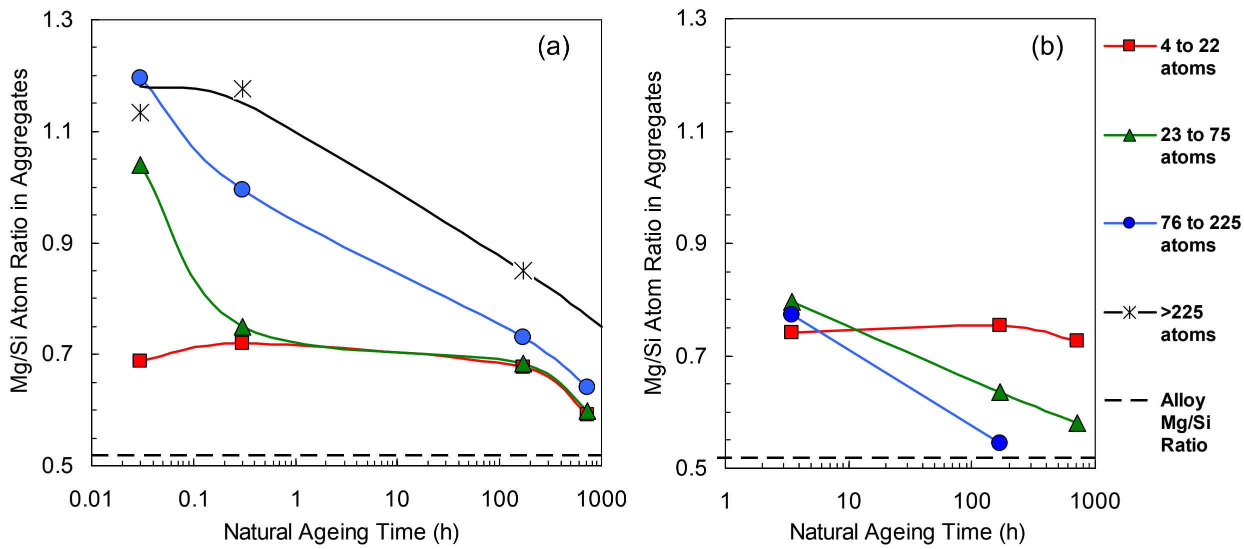

Fig. 6: Effect of natural ageing on the Mg/Si ratios in variously sized solute aggregates in (a) T6 and (b) T4 conditions, calculated from sums of Mg and Si in all aggregates containing both Mg and Si.

Figure 6 demonstrates that the Mg/Si ratio increases with increasing solute aggregate size across most heat treatment conditions. Cluster 1 was not included because Mg/Si ratios are not meaningful for such small clusters. The rate of increase in Mg/Si ratio and the actual values are different for different natural ageing conditions. There is, for example, a trend towards lower Mg/Si ratios with increasing natural ageing time in both the T4 and T6 conditions. It is evident from Fig. 6 that higher T6 (but not T4) strengths are associated with higher average solute aggregate Mg/Si ratios. Of particular note is the fact that in the highest yield strength condition (245 MPa), the Mg/Si ratio of not only the precipitates, but also of the zones and the largest clusters (Cluster 3), is close to 1.1. These results suggest that the cluster Mg/Si ratio is important in determining both suitable precipitation conditions for β" and the final strength of the alloy.

It is important to note that the Mg/Si ratios here were not determined for each individual solute aggregate and then averaged, but rather by dividing the total number of detected Mg atoms by the total number of Si atoms in each solute aggregate category – only for aggregates containing both Mg and Si (i.e. excluding Si-Si, Mg-Mg and Cu-Cu clusters). As with all statistical analyses, the results depend on both the quality and the quantity of the data. Table 3 gives an impression of the amount of data that the results in Figs. 3-6 are based on and suggests that while the statistics for the small aggregates are great, the large ones are at times under-represented and therefore prone to more scatter.

4. Summary

Solute aggregates occurring in naturally aged and under-aged 6xxx alloys have been detected by 3D atom probe and actual total numbers of atoms were approximately categorised into precipitates (>500 atoms), coherent zones (167-500 atoms) and three differently sized clusters (<167 atoms) in order to understand their respective contributions to the yield strength. The following conclusions are made: (a) clusters with <167 atoms play a significant role in determining the alloy strength not only by making their own hardening contribution, but also more indirectly by determining suitable precipitation conditions for β", and (b) the cluster Mg/Si ratio is important in explaining the formation of β" and thus the detrimental effect of natural ageing. The highest T6 strengths are associated with Mg/Si ratios of ≥1 in large clusters (51-166 atoms), zones (167-500 atoms) and precipitates.

Acknowledgements

The authors would like to thank the Aluminium Corporation of China (CHALCO) for supporting this work financially and for providing materials as part of the Australia-China International Centre for Light Alloys Research (ICLAR). The assistance of Dr X.Y. Xiong with 3DAP analysis at the Monash Centre for Electron Microscopy (MCEM) and the provision of the TEM results in Fig. 1 by Mr Sam X. Gao are also gratefully acknowledged.

References

[1] H. R. Shercliff and M. F. Ashby: Acta Metall. Mater. 37 (1990) 1789-1802.
[2] P. A. Rometsch and G. B. Schaffer: Mater. Sci. Eng. A 325 (2002) 424-434.
[3] S. Esmaeili, D. J. Lloyd and W. J. Poole: Acta Mater. 51 (2003) 3467-3481.
[4] B. Raeisinia, W. J. Poole, X. Wang and D. J. Lloyd: Metall. Mater. Trans. 37A (2006) 1183-1190.
[5] M. Murayama and K. Hono: Acta Mater. 47 (1999) 1537-1548.
[6] M. Murayama, K. Hono, W. F. Miao and D. E. Laughlin: Metall. Mater. Trans. 32A (2001) 239-246.
[7] J. Buha, R. N. Lumley, A. G. Crosky and K. Hono: Acta Mater. 55 (2007) 3015-3024.
[8] J. Buha, R. N. Lumley and A. G. Crosky: Phil. Mag. 88 (2008) 373-390.
[9] L. Cao, P. A. Rometsch, H. Zhong, Y. Mulji, X. Gao, B. C. Muddle: The 12th International Conference on Aluminium Alloys (2010) in press.